Analytica Chimica Acta 1110 (2020) 98–108

Contents lists available at ScienceDirect

Analytica Chimica Acta

journal homepage: www.elsevier.com/locate/aca

An ultrasensitive label-free colorimetric biosensor for the detection of glucose based on glucose oxidase-like activity of nanolayered manganese-calcium oxide

Samaneh Rashtbari [a], Gholamreza Dehghan [a, *], Mojtaba Amini [b]

[a] Department of Biology, Faculty of Natural Sciences, University of Tabriz, Tabriz, Iran
[b] Department of Chemistry, Faculty of Science, University of Maragheh, Maragheh, Iran

HIGHLIGHTS

- Glucose oxidase-like activity of NL-$MnCaO_2$ was investigated using colorimetric method.
- An enzyme free biosensor for the detection of glucose in real samples was developed.
- Catalytic efficiency of NL-$MnCaO_2$ was dependent on pH and temperature.
- NL-$MnCaO_2$ is a multi-functional enzyme mimetic nanostructure which can be used in various fields of biomedicine.

GRAPHICAL ABSTRACT

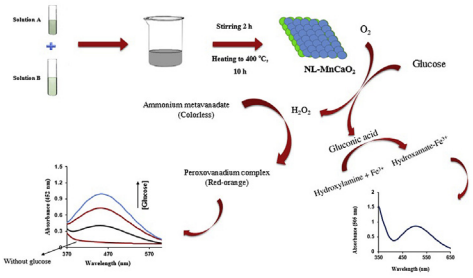

ARTICLE INFO

Article history:
Received 15 January 2020
Received in revised form
4 March 2020
Accepted 10 March 2020
Available online 13 March 2020

Keywords:
Nanolayered $MnCaO_2$
Mimic activity
Biosensor
Enzyme free
Glucose determination

ABSTRACT

During the last years, enzyme-based biosensors have gained much more attention among the researchers and have had great success in the determination of different biological macromolecules. Nanomaterials with intrinsic enzyme-mimic activity are widely used in biomedicine as artificial enzymes. Here, we report glucose oxidase-mimic activity of nanolayered manganese-calcium (Mn–Ca) oxide nanoparticles (NL-$MnCaO_2$). In this work, NL-$MnCaO_2$nanoparticles were synthesized and characterized using different techniques including transmission electron microscopy (TEM), scanning electron microscopy (SEM), fourier-transform infrared spectroscopy (FTIR) and powder X-ray diffraction (XRD). Also, the ability of these compounds for the glucose and hydrogen peroxide (H_2O_2) determination was investigated. A non-enzymatic strategy for the colorimetric detection of glucose and H_2O_2 was reported which can be utilized not only for the rapid detection and analysis of glucose by the naked eye but also the quantitative assay of glucose by spectrophotometry. The in situ generated H_2O_2 and gluconic acid (GA) from the oxidation of glucose through the glucose oxidase-mimicking activity of NL-$MnCaO_2$ was detected using a colorimetric method. Also, the results confirmed the application of these compounds for the detection of glucose in human serum samples with a detection limit (LOD) of 6.12×10^{-6} M. The results showed that NL-$MnCaO_2$ can be used as an alternative for the natural enzymes and act as a simple, sensitive and enzyme-free biosensor for the detection of glucose in real samples. The proposed strategy shows some advantages including sensitivity, short detection time and low detection limit.

* Corresponding author.
E-mail addresses: dehghan2001d@yahoo.com, gdehghan@tabrizu.ac.ir (G. Dehghan).

https://doi.org/10.1016/j.aca.2020.03.021
0003-2670/

1. Introduction

Natural enzymes are catalysts that can speed up chemical reactions rate by reducing activation energy and mediated the biological processes under mild conditions [1]. However, these biomolecules have some drawbacks including the high cost of synthesis, purification and low stability in extreme conditions of pH or temperatures for performing catalytic functions [2,3]. Therefore, developing efficient artificial enzymes, as alternatives to natural enzymes, using non-protein molecules such as metal-complexes, metal-nanomaterials, polymeric and supramolecules become an interesting field for researchers [4].

Nano-based materials due to their physicochemical properties relative to bulk materials including large surface/volume ratios (because of their small size), optically active, mechanically strong and chemically reactive (which are often absent in the bulk materials) have various applications in different areas including biosensing, catalysis, textile industry, drug delivery and water treatment [5–7]. Enzyme mimetic behavior of some nanomaterials is one of the most interesting features of these materials which make nanomaterials as potential alternatives for natural enzymes. Nanomaterials, with enzyme mimic activities (nanozymes), have gained much more attention among the researchers during the past decades because of their unique properties such as low-cost, high stability and simple preparation. Also, nanozymes have their catalytic activity even in the harsh environmental conditions of pH and temperatures [8]. Various studies have reported enzyme mimic activity of different nanomaterials with diverse structures [4,9–27]. The reported enzyme-like activities for nano-sized materials includes the superoxide dismutase-like (SOD like), oxidase-like, catalase-like and peroxidase-like activities. Also, there are few reports about glucose oxidase-like activity of nanoparticles [2,28,29]. Some studies reported that nanozymes with peroxidase or oxidase-like activities can be used for the detection of glucose in the presence and absence of H_2O_2, respectively. These nanoenzymes oxidize TMB (3,3′,5,5′-tetramethylbenzidine) and ABTS (2,2′-azino-bis(3-ethylbenzothiazoline-6-sulphonic acid)-diammonium salt), as peroxidase substrates. In such systems, glucose oxidase is used for the generation of H_2O_2 and the resulting H_2O_2 is then utilized to oxidize chromogenic substrates (TMB and ABTS) by nanozymes [4,9,30,31].

Mixed metal oxide nanomaterials are used in various areas of chemistry and physics. When two metals combine together in an oxide matrix, acquire unique electronic and magnetic properties can be observed which could not be seen in each metal alone. The most common use of mixed metal oxide nanomaterials is in the area of catalysts [32]. In the chemical reactions, mangenese (Mn) oxides were widely used as efficient catalysts for oxidation of different organic and inorganic compounds; e.g. selective oxidation of alcohols to aldehydes in the presence of O_2. Mn oxides due to their low cost, physical and chemical properties and being environmentally friendly are the most attractive inorganic compounds [33–36]. These compounds can be synthesized, as nano-sized nanostructures, easily using various methods. Among the functional materials, the metallic oxides (in the nanometric scale) such as Mnoxide nanoparticles have gained much more attention due to their unique properties and the role of Mn as a regulatory cofactor for some main enzymes and receptors (its physiological function). Different studies have been reported the nanolayered Mn oxides (among various Mn oxides) as efficient catalysts in oxidation reactions.

The rapid and accurate determination of the blood glucose level is one of the most important issues in medical and pharmaceutical research, particularly for diagnosing diabetes mellitus. Also, detection of the glucose concentration has a vital role in the fermentation industry, biotechnology, food industry and environmental protection [37,38]. Diabetes mellitus is a chronic disease in which glucose level in blood is higher than normal and this can result in various disorders. So, the accurate and proper detection of the glucose concentration can reduce the risk of some disorders such as diabetes, kidney failure, atherosclerosis and nerve degeneration [39]. In this regard, developing a fast, sensitive and simple biosensor to determine the blood glucose level has gained considerable attention among the researchers during the past few years. The glucose oxidase based biosensors for glucose detection have some disadvantages, including low efficiency, complicated immobilization procedure, high enzyme costs, critical operating conditions, instability, etc. [40,41]. To overcome these drawbacks, many researchers are trying to develop enzyme-free glucose sensors using different nanomaterials, including nanowires, nanorods, nanosheets, nanoparticles and nanotubes due to their unique structural, physical and functional properties [41]. Various studies have reported enzyme-free colorimetric detection methods based on nanozymes for determination of glucose [28,42–49].

In the current study, we reported a glucose oxidase-like activity of nanolayered manganese-calcium (Mn–Ca) oxide (NL-$MnCaO_2$) for the first time. We found that this compound is able to catalytically oxidize glucose and produce gluconate and hydrogen peroxide (H_2O_2), similar to glucose oxidase. As glucose plays the main role in various physiological activities, NL-$MnCaO_2$catalyzed glucose oxidation can be important in both theoretical and applied types of research. Also, the application of this compound for the determination of glucose in the real samples was investigated, too. Therefore, we presented a non-enzymatic strategy for the colorimetric detection of glucose, where the oxidation of glucose and the colorimetric detection of H_2O_2were simultaneously conducted under the catalysis of the single nanoezyme (NL-$MnCaO_2$). The proposed method can be utilized not only for the rapid detection and analysis of glucose by the naked eye but also for the quantitative assay of glucose by spectrophotometry.

2. Materials and methods

2.1. Chemical and materials

Hydrogen peroxide (H_2O_2, 30%), 3,3′,5,5′-tetramethylbenzidine(TMB), ammonium metavanadate (AV), dimethyl sulfoxide (DMSO), $CaCl_2{\cdot}4H_2O$, $Mn(CH_3COO)_2{\cdot}4H_2O$, $KMnO_4$, KOH and $FeCl_3{\cdot}6H_2O$were obtained from Sigma-Aldrich and were used without further purification. Sodium acetate (MW: 82.03 g/mol), acetic acid (MW: 60.05 g/mol), Ethylenediaminetetraacetic acid (EDTA), trimethylamine (Et_3N), trichloroaceticacid (CCl_3COOH), HCl, glucose, fructose, galactose and maltose were purchased from Merck (Darmstadt, Germany). Hydroxylamine hydrochloride ($NH_2OH{\cdot}HCl$) was obtained from Fluka (Steinheim, Germany). All solvents and reagents were used without further purification.

Glucose stock solution (5.5×10^{-3} M) was prepared by dissolving an appropriate amount of its powder in distilled water. Acetate buffer solution (1.0×10^{-2} M) was prepared by dissolving a 0.424 g of sodium acetate and a 0.02 g of acetic acid in 300 mL distilled water. Then, the pH level of the buffer was adjusted to 5.0 using HCl or NaOH and the final volume was made up to 500 mL by adding distilled water. TMB stock solution (1.04×10^{-3} M) was prepared by dissolving a desired amount of its powder in DMSO.

2.2. Synthesis of nanolayered mixed metal oxides (NL-$MnCaO_2$)

Our previously reported method was used for the synthesis of nanolayered mixed metal oxides (NL-$MnCaO_2$) [33]. Briefly, a

2.70 mmol $CaCl_2 \cdot 4H_2O$ and a 5.6 mmol $Mn(CH_3COO)_2 \cdot 4H_2O$ solutions were mixed in 5 mL water (solution A). To a solution of $KMnO_4$ (2.4 mmol, 379 mg) in 100 mL water, KOH (17.0 g) was added to obtain a hot KOH–$KMnO_4$ solution (solution B). Solution A was added to solution B under vigorous stirring resulted in a dark precipitate. Then the mixture was allowed to cool with continued stirring for 2 h. The obtained suspension was filtered and washed with distilled water (3 L) before being allowed to dry for 12 h at 60 °C in an oven. Then the solid was heated to 400 °C for 10 h in the air to obtain a brown powder.

2.3. Characterization of NL-$MnCaO_2$

The morphology of NL-$MnCaO_2$was characterized using scanning electron microscopy (SEM, LEO 1430VP) and transmission electron microscopy (TEM, Philips CM120) at an accelerating voltage of 200 kV. All UV–vis absorption spectroscopy measurements were performed using a UV–vis spectrophotometer (T60, PG Instruments LTD., Leicestershire, UK) in a quartz cell of 1 cm path length. A Bruker, D8 ADVANCE diffractometer (Cu–K -radiation) (Germany) was used for recording X-ray powder patterns of NL-$MnCaO_2$ in the range of $2\theta = 10–70$. The following procedure was used to prepare the samples for XRD analysis: briefly, a 20 μL of NL-$MnCaO_2$ suspension was dropped on a silicon wafer. After drying at 60 °C, the formed evident film was used for XRD analysis. All FTIR spectra of NL-$MnCaO_2$were recorded on a Bruker vector 22 after mixing the samples with KBr in the range of 400–4000 cm^{-1}. A microprocessor pH meter (HANA Instruments-USA) equipped with a glass electrode was applied for the determination of the pH value of the all prepared solutions.

2.4. Oxidase-like activity of NL-$MnCaO_2$ and apparent kinetic assays

To investigate the oxidase-like activity of NL-$MnCaO_2$, the TMB (in DMSO, 1.04 mM) was used as a substrate and changes in the absorption spectra of TMB were detected at 652 nm. Similar to oxidases, NL-$MnCaO_2$ can catalyze the oxidation of TMB in the absence of H_2O_2 and produce a blue-colored product which has a maximum absorbance peak at 652 nm. Kinetic analyses were performed in 2.0 mL acetate buffer solution (HAc-NaAc, 0.01 M, pH 5.0), different concentrations of TMB as the substrate (2.6, 5.2, 7.8, 10.4, 13, 15.6, 18.2 and 20.8 μM) and a fixed concentration (100 μL) of 2.0 mg/mL NL-$MnCaO_2$. The final volume of the solution was reached to 4.0×10^{-3} L using HAc-NaAc buffer solution and the reactions were carried out at 25 °C (at room temperature) and the absorbance changes at 652 nm were recorded. The obtained data were fitted to the Michaelis–Menten equation and, then, the apparent kinetic parameters (K_m andV_{max}) were calculated using the respective Lineweaver-Burk plots and equation (1):

$$\frac{1}{V} = \frac{K_m}{V_{\max}} \cdot \frac{1}{[S]} + \frac{1}{V_{\max}} \quad (1)$$

where V, K_m,$V_{\max}$ and $[S]$ denote the reaction initial velocity, the Michaelis constant, the maximal reaction velocity and the concentration of TMB.

2.5. Glucose oxidase-like activity of NL-$MnCaO_2$ and apparent kinetic assays

To determine the glucose oxidase-like activity of NL-$MnCaO_2$, a solution of glucose with different concentrations (2.7, 13.7, 27.5, 41.2, 55, 68.7, 82.5, 96.2, 110 and 123.7 μM) was mixed with a 100 μL of 2.0 mg/mL NL-$MnCaO_2$ in 2.0 mL HAc-NaAc buffer solution (0.01 M, pH 5.0). The final volume of the solutions were reached to 4.0×10^{-3} L using HAc-NaAc buffer solution and were incubated for 60 min. The amount of gluconic acid (GA) was determined by the reaction between GA and hydroxylamine and Fe^{3+}. The hydroxamate-Fe^{3+} complex formation can cause a change in the color of the reaction solution toward red, with maximum absorption at 505 nm. In detail, 250 μL of solution A (containing 0.15 mM Et_3N and 5 mM EDTA in distilled water) and 25 μL of solution B (3M NH_2OH in distilled water) were mixed with the catalytic reaction solution and the obtained mixture was incubated for 15 min. After this time, 125 mL of solution C (1 M HCl, 0.1 M $FeCl_3$ and 0.25 M CCl_3COOH in distilled water) was added to the reaction mixture and incubated for 5 min [50,51].

Assay for determining H_2O_2 (the other possible product) was carried out using a colorimetric reaction between H_2O_2 and ammonium metavanadate(AV) [52]. The principle of this colorimetric method is based on the peroxovanadium complex (a red-orange complex) formation under the acidic condition with maximum absorption at 452 nm. Briefly, a 0.01 M AV solution was prepared by dissolving 0.1162 g of AV powder in 100 mL of 0.5 M sulfuric acid. The prepared solution was added to the solutions containing different concentrations of glucose and a fixed concentration of NL-$MnCaO_2$ and the absorption peak of the solutions was recorded at 452 nm. Kinetic analyses were performed using equation (1).

2.6. Detection of glucose

Under the optimum condition, the detection of glucose was carried out using glucose oxidase-like activity of NL-$MnCaO_2$. For this purpose, different concentrations of glucose (0, 18.3, 55, 91.6, 128.3, 165, 201.6, 238.3, 275, 311.6, 348.3, 385, 421.6, 458.3, 495, 531.6 and 600 μM) were mixed with a 100 μL of 2.0 mg/mL NL-$MnCaO_2$. The final volume of the solutions were reached to 4.0×10^{-3} L using HAc-NaAc buffer solution and were incubated for 60 min. Then, the detection of glucose was performed spectrophotometrically using a colorimetric method as described in section 2.5. In detail, the reaction solutions containing fixed concentrations of AV and NL-$MnCaO_2$ and additional concentrations of glucose were incubated for 60 min. Then, the absorption spectra of samples were measured at 452 nm. Limit of detection (LOD) was calculated based on the method of SD of the response and the slope. LOD was calculated by the formula of $LOD = 3\ \sigma/S$, where σ is the standard deviation of the blank and S is the slope of the calibration curve.

Selectivity studies were performed using different glucose analogues (instead of glucose) such as fructose (2 mM), galactose (2 mM) and maltose (2 mM). Then, the absorption spectra of samples were measured at 452 nm.

2.7. Determination of glucose in spiked human serum samples

The experiments were also performed by using serum as the media. For the determination of blood glucose in real samples, healthy human plasma was prepared from the Iranian Blood Transfusion Organization (IBTO). After deproteinization process, healthy human serum samples were spiked with various concentrations of glucose. In detail, the deproteinization process was carried out using acetonitrile [53]. In detail, 1.5×10^{-3} L acetonitrile was added to the previously spiked serum samples (0.5×10^{-3} L) and then centrifuged at 13000 rpm for 5 min. After removing proteins, the prepared supernatant was used for further analyses. The same procedure as described in sections 2.5 and 2.6 were used to analyze the unspiked and spiked serum samples for detection of glucose. Calibration curve was constructed by plotting the peak

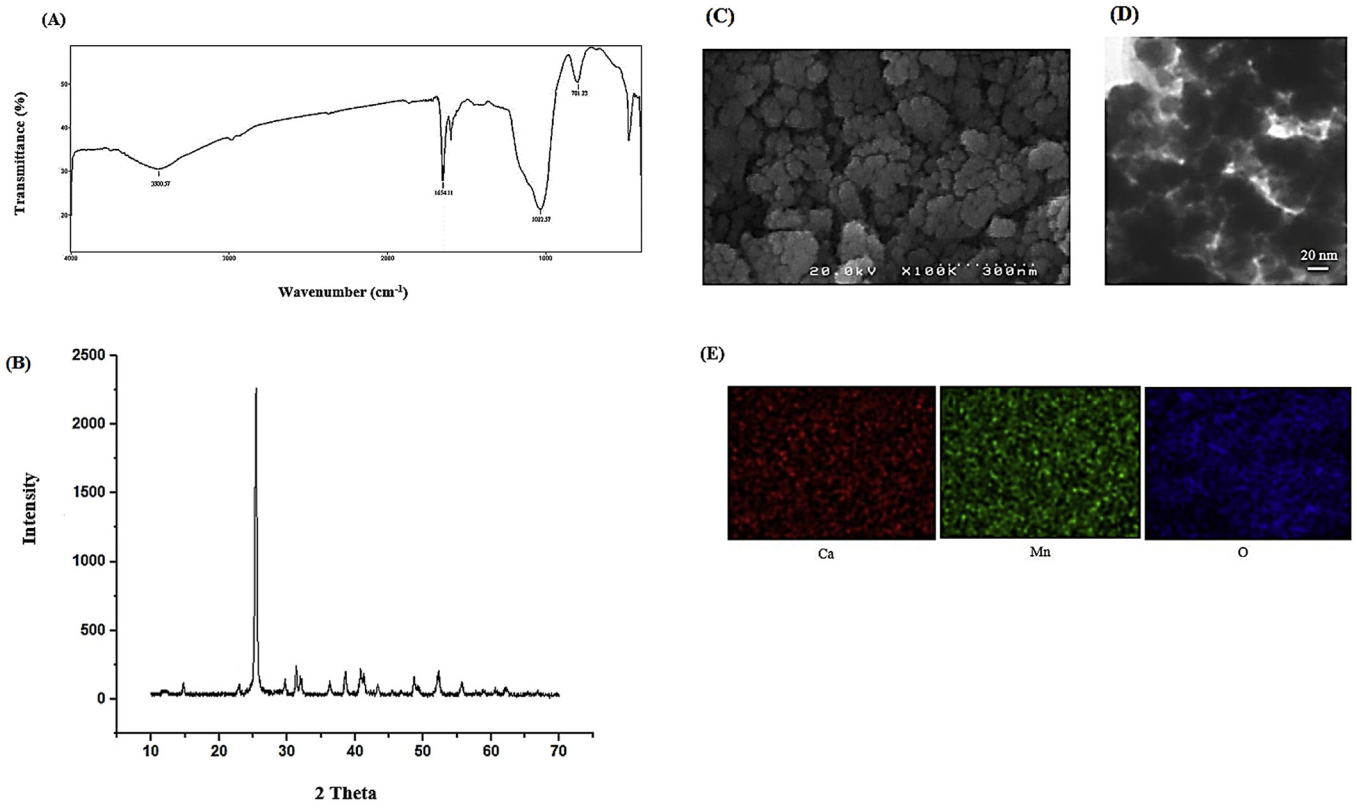

Fig. 1. FTIR spectra of NL-$MnCaO_2$(A), XRD patterns of NL-$MnCaO_2$ (B), SEM (C) and TEM (D) images of nano-sized Mn–Ca oxide. Elemental mapping of Ca, Mn and O (E).

areas of samples at 452 nm against the glucose concentrations. LOD was calculated as mentioned in section 2.6. The added-found procedure was applied to investigate the accuracy and precision of the proposed method for determination of glucose in serum samples. For this purpose, a series of five serum sample solutions with the glucose concentrations of 10, 45 and 80 $\times$ 10^{-6} M were prepared and the same procedure as described in section 2.5 was used to analyze the prepared samples. The relative standard deviation (RSD) and recoveries values were calculated. RSD% was obtained using the formula of RSD% =(S/X) $\times$ 100, where S is the standard deviation of five analyses and X is the average (mean) of data values and the recoveries values were calculated by dividing the found amount to the added amount.

3. Results and discussion

3.1. Characterization of NL-$MnCaO_2$

Synthesizing of NL-$MnCaO_2$by the reaction of $KMnO_4$, Mn(II)$(OAc)_2$ and $CaCl_2$ in the presence of KOH is a simple and cheap procedure. Different techniques including FTIR spectroscopy, XRD patterns, TEM and SEM were used for the characterization of the synthesized NL-$MnCaO_2$. In FTIR spectra of NL-$MnCaO_2$, broad bands related to the O–H stretching and H–O–H bending vibrational spectra are observed at ~3200-3500 cm^{-1} and ~1360 cm^{-1}, respectively. The observed peak at ~700 cm^{-1} is related to Mn–O–Mn bonds (Fig. 1A) [54–56].

In XRD patterns of these compounds a peak near the $2\theta = 38$ was observed which exist in all octahedrally coordinated Mn oxide materials. Also, the peaks near $2\theta = 11$, 25 and 36 were observed in XRD patterns of NL-$MnCaO_2$which are observed in most layered materials, e.g. layered oxides (Fig. 1B) [54–56]. Also, morphological studies of the prepared oxides were carried out using SEM and TEM. The SEM and TEM images are shown in Fig. 1C and 1D. These images represent aggregated nanoparticles and morphology similar to a crumpled paper. EDX-Mapping images show the homogeneous elemental distributions (Fig. 1E).

3.2. Optimization of experimental conditions

Certainly, the catalytic activity of NL-$MnCaO_2$ (like other enzyme mimetic nanomaterials) is dependent on the temperature and pH. So, the effects of different temperatures and pH values on the catalytic efficiency of NL-$MnCaO_2$ were investigated to optimize experimental conditions. The enzyme mimetic activity of NL-$MnCaO_2$ was studied at different temperatures from 20 °C to 50 °C and various pH values from 2.0 to 9.0 by incubating NL-$MnCaO_2$(100 μL), TMB (11 μM) and H_2O_2 (48 μM) for 5 min. The results revealed that NL-$MnCaO_2$ can mimic oxidase activity at pH 5.0 and 25 °C (Fig. 2A–B). Therefore, these values were used for further studies. In general, optimum conditions resulted in the generation of small, high crystalline and monodispersed particles. So, it can be considered that in the optimized condition (pH 5.0 and 25 °C) dispersion of NL-$MnCaO_2$ can completely occur and the maximum surface active sites of particles exposed to the substrate molecules. Also, generation of small sized particles could increase the surface/volume ratios. So, with increasing the surface area, the catalytic activity of nanoparticle increase, too [57].

3.3. Oxidase and glucose oxidase-like activities of NL-$MnCaO_2$

The oxidase-like activity of NL-$MnCaO_2$ was investigated using TMB as the substrate in the absence of H_2O_2. The obtained results revealed that NL-$MnCaO_2$ can oxidize TMB in a concentration and

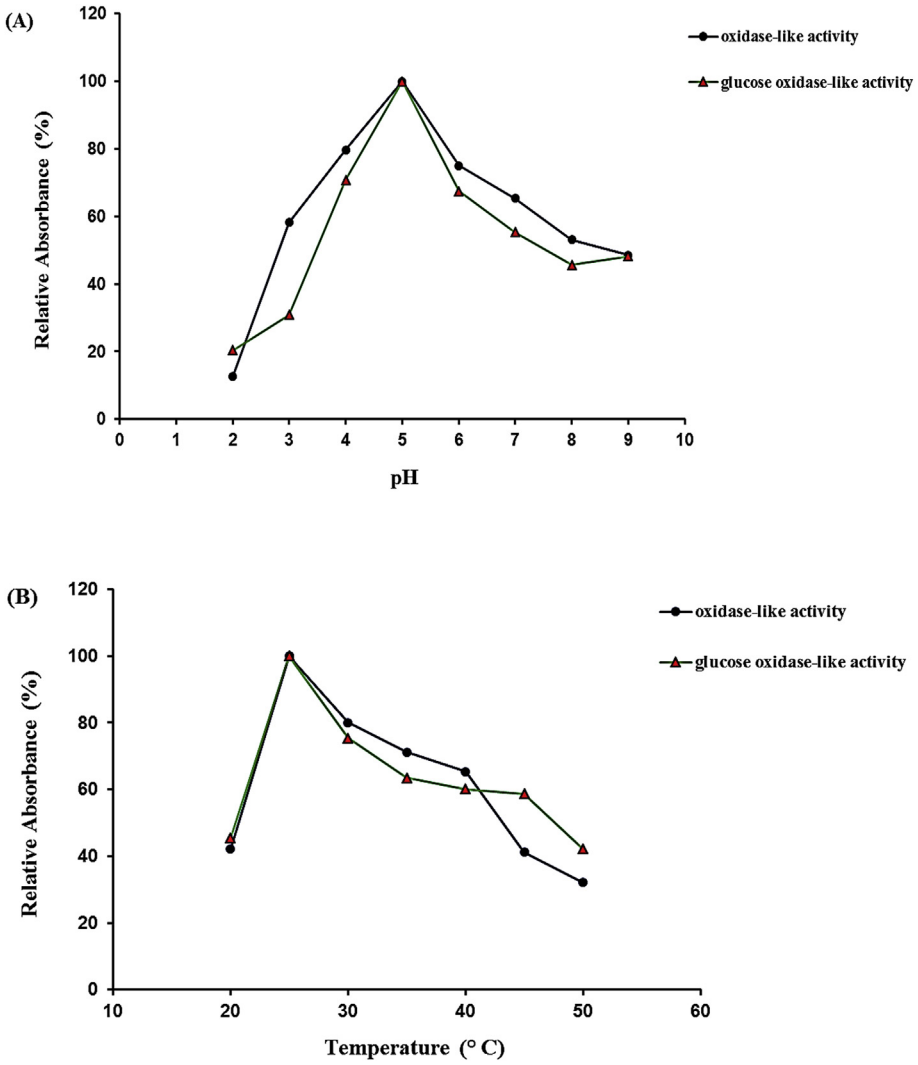

Fig. 2. Effects of pH (A) and temperature (B) on catalytic activity of NL-$MnCaO_2$.

time-dependent manner and produce a blue-colored product which has a maximum absorbance peak at 652 nm (Fig. 3A and B). Then, the apparent kinetic parameters were calculated for NL-$MnCaO_2$in the presence of TMB. Michaelis-Menten and Lineweaver-Burk curves were established (Fig. 3C) and kinetic parameters, V_{max} and K_m, were calculated to be 97.83×10^{-8} Ms^{-1} and 0.087×10^{-3} M, respectively.

Moreover, we investigated the ability of NL-$MnCaO_2$ to oxidize glucose (glucose oxidase-mimicking activity). For this purpose, NL-$MnCaO_2$ was incubated with glucose under optimum condition. After 60 min, the production of GA, as a reaction product, was assessed using a colorimetric assay. In detail, with adding Fe^{3+} and hydroxylamine to the reaction solution the color of the solution changed to red, with a maximum absorbance peak at 505 nm. These results indicated that GA was produced during the reaction catalyzed by NL-$MnCaO_2$ and confirmed the glucose oxidase-like activity of NL-$MnCaO_2$ [50].

The other product, hydrogen peroxide (H_2O_2), was assessed using a colorimetric method. In detail, when ammonium metavanadate (AV) was added to the reaction solution and react with H_2O_2 under acidic condition, the color of the solution was changed and turned red-orange due to peroxovanadium complex formation with a maximum absorption peak at 452 nm (Fig. 4A). As shown in Fig. 4B, the color of the resulting solution changed after adding AV, which confirmed the production of H_2O_2 due to the glucose oxidase-mimicking activity of NL-$MnCaO_2$. Also, control studies were carried out either without NL-$MnCaO_2$ or without glucose (Fig. 4B) and negligible color changes in the reaction mixtures observed. The obtained results confirmed the production of H_2O_2 because of the glucose oxidase-mimicking activity of NL-$MnCaO_2$ and H_2O_2 generation increased with increasing glucose concentration. Michaelis-Menten and Lineweaver-Burk double reciprocal curves were established (Fig. 4C). Then, the apparent kinetic parameters, V_{max} and K_m, for the reaction of NL-$MnCaO_2$ with glucose were calculated to be 58.8×10^{-4} Ms^{-1} and 0.019×10^{-3} M, respectively. In comparison with the natural enzyme (glucose oxidase) with K_m value of 2.6×10^{-3} M [58], the NL-$MnCaO_2$ has a relatively lower (but comparable) K_m value, suggesting relatively high affinity of NL-$MnCaO_2$ for glucose.

3.4. Colorimetric detection of glucose and H_2O_2 using NL-$MnCaO_2$

As mentioned above, NL-$MnCaO_2$ can oxidize glucose with its glucose oxidase-like activity and produce H_2O_2. As mentioned in section 2.5, the reaction between H_2O_2 and AV produces a red-orange colored complex with maximum absorption at 452 nm.

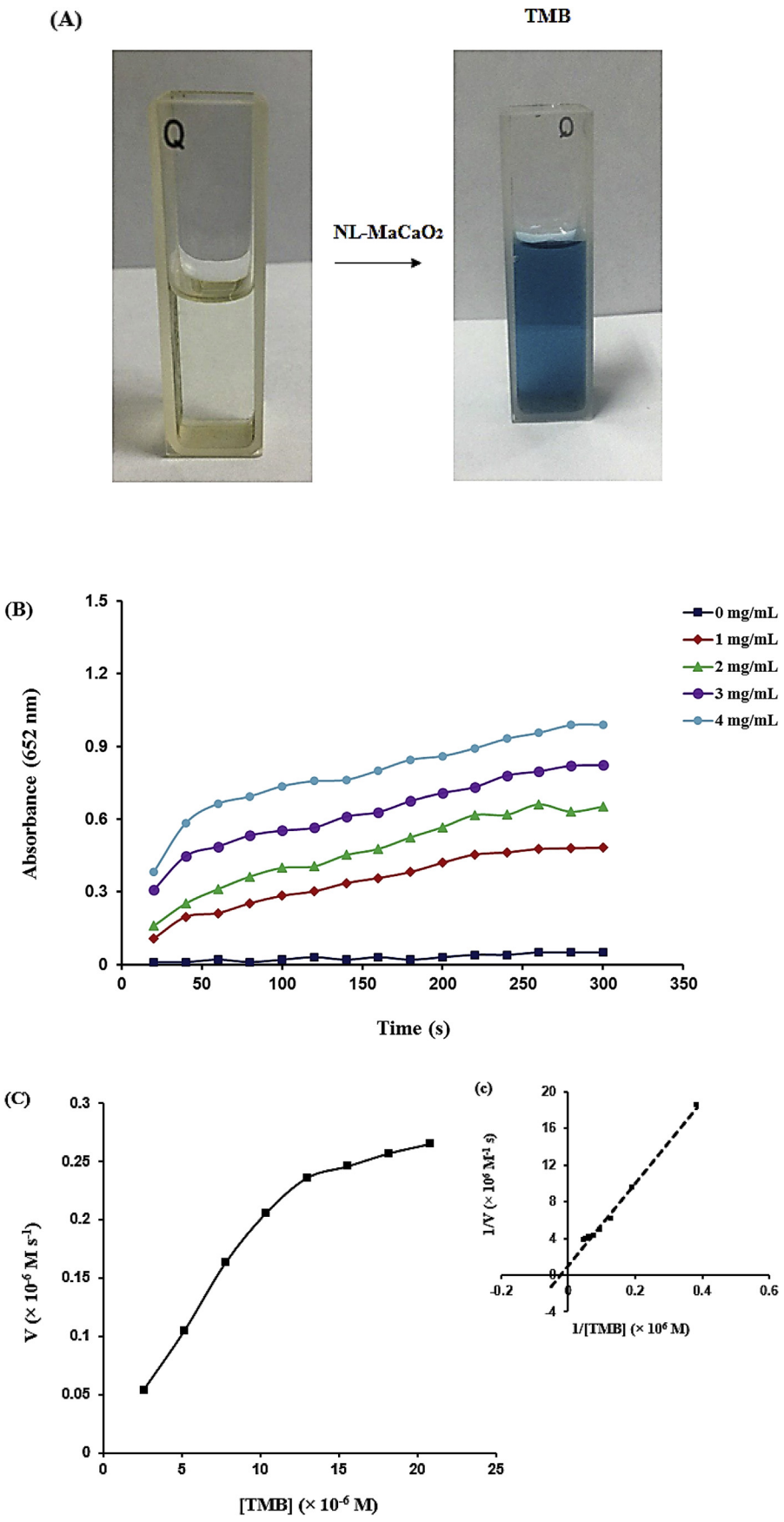

Fig. 3. The color evolution of TMB oxidation catalyzed by NL-$MnCaO_2$in the absence of H_2O_2(A) and concentration and time-dependent absorbance change at 652 nm in the absence or presence of different concentrations of NL-$MnCaO_2$(B) and kinetics for oxidase-like activity of NL-$MnCaO_2$ in the presence of TMB as substrate (C).

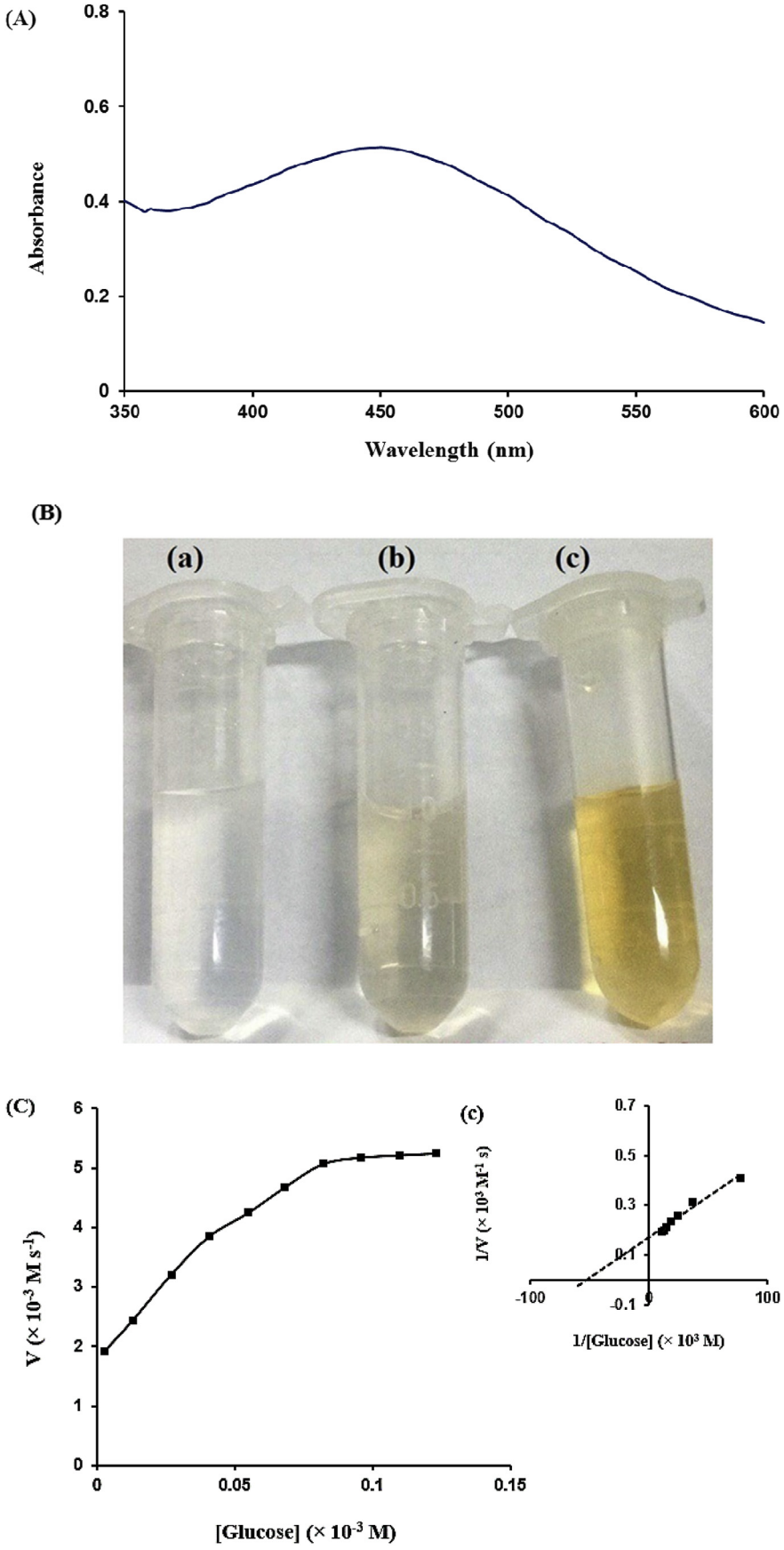

Fig. 4. UV–vis absorption spectra obtained from samples containing H_2O_2 and AV (A), NL-$MnCaO_2$ catalyze the oxidation of glucose to gluconic acid, producing a red-orange colored product (Glucose and AV in the absence of NL-$MnCaO_2$ (a) NL-$MnCaO_2$ and AV in the absence of glucose (b) and NL-$MnCaO_2$ in the presence of glucose (c)) (B) and kinetics for glucose oxidase-like activity of NL-$MnCaO_2$ in the presence of glucose as substrate (C).

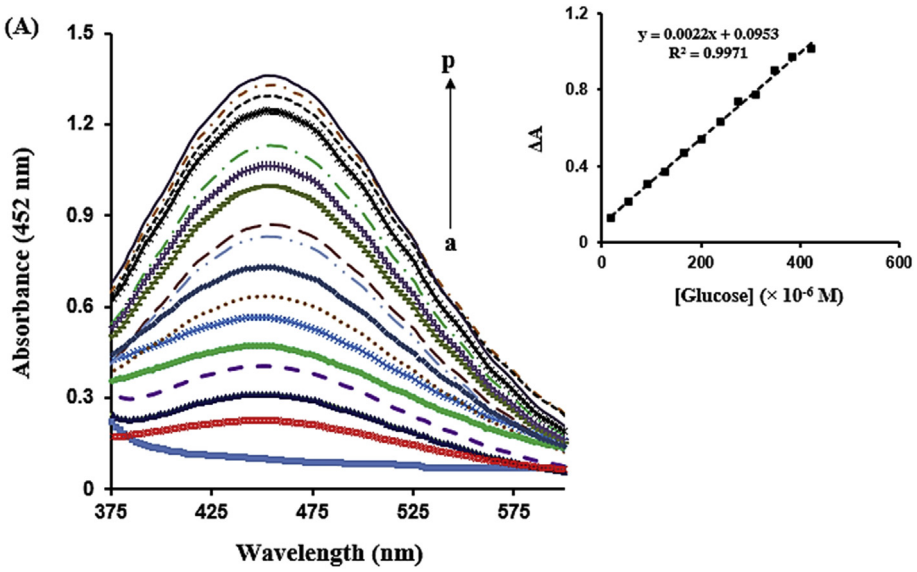

Fig. 5. The absorption spectra of NL-$MnCaO_2$ and AV system upon adding various concentrations of glucose (0–400 μM, from bottom to top) (A) and the linear relationship between the absorption intensities and the concentration of glucose (B).

Table 1
Comparison of the proposed approach with some other systems for H_2O_2 and glucose detection.

Materials	Actual samples	Signal output	LOD (μM)	Linear range (mM)	Ref.
Au@Ag NRs	–	Colorimetric	39	0.05–20	[60]
Tb^{3+}-phen-AgNPs	Human serum	Photoluminescence (Fluorescence quenching)	0.019	0.00005–0.009	[53]
AuNPs	–	Colorimetric	49	0.1–1	[49]
Chitosan–Au	Human serum	Colorimetric	3	0.006–0.14	[61]
RhNPs	Human serum	Colorimetric	0.75	0.005–0.125	[62]
Polyaniline nanotubes-GOx	Human urine	Electrochemical	0.3	0.01–5.5	[63]
RGO-CdS-CoOx nanocomposite	Human serum	Electrochemical	0.4	0–1	[64]
CdTe QDs silica nanoparticles	Human serum and urine	Photoluminescence	1.93	0.005–0.4	[65]
Co_3O_4@CeO_2	–	Colorimetric	1.9	0.001–0.075	[66]
MnSe	–	Colorimetric	0.085	0.00017–0.01	[67]
Fe_3O_4 NPs	–	Colorimetric	30	0.005–0.1	[68]
CdSe–ZnS QDs-GOx	–	Photoluminescence	–	0.2–10	[69]
Fe3O4 nanoparticles	Human serum	Spectrophotometry	50	0.05–4	[70]
NL-$MnCaO_2$	Human serum	Colorimetric	23.86	0.0183–0.421	Present work

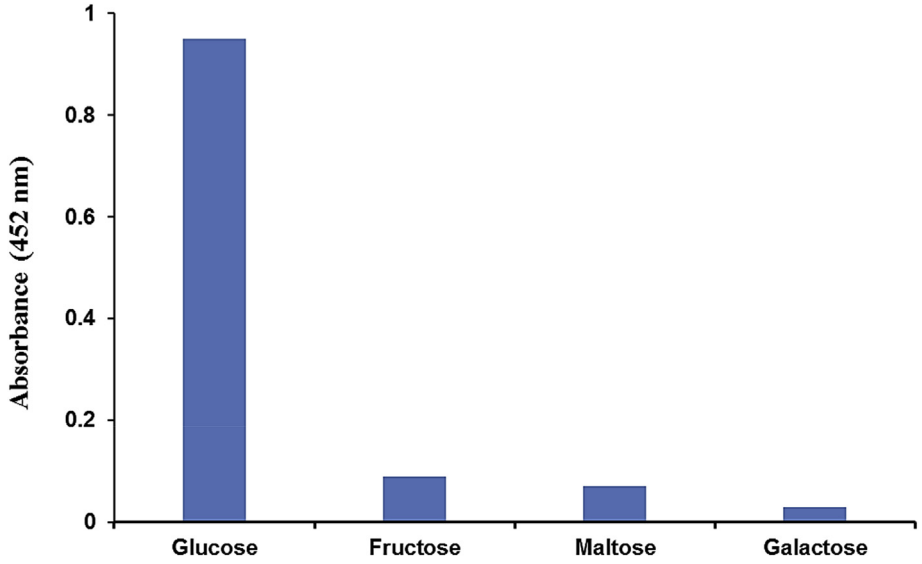

Fig. 6. Selectivity of the proposed method for the glucose detection.

Table 2
Determination of glucose in serum sample.

amount added ($\times 10^{-6}$ M)	amount found ($\times 10^{-6}$ M)	Recovery (%)	RSD (%)
10	10.89 ± 1.66	108.9	1.682
45	47.84 ± 0.66	106.3	0.722
80	76.32 ± 1.09	95.4	1.225

So, the sensitive H_2O_2 response of the proposed system made it possible for detecting glucose. As shown in Fig. 5A, the absorbance at 452 nm increased gradually with rising the concentration of glucose up to 600 μM. A good linearity ($R^2 = 0.9971$) was observed in the concentration range of 18.3–421.6 μM (Fig. 5B). The LOD of glucose was obtained 23.86 μM which is comparable or even superior to those achieved by using some other nanoparticles (Table 1).

Using the standard addition method, the concentration of generated H_2O_2 during the glucose oxidase-like activity of NL-$MnCaO_2$ were calculated. The obtained results indicated that with increasing the concentration of glucose, H_2O_2 concentration was increased, too.

3.5. Glucose detection mechanism

The following equations show the glucose catalytic reaction and generation of H_2O_2 by NL-$MnCaO_2$:

$$O_2 + glu\cos e \xrightarrow{NL-MnCaO_2} H_2O_2 + Gluconicacid \quad (2)$$

$$H_2O_2 + NH_4VO_3 + H_2SO_4 \rightarrow NH_4[VO(O_2)SO_4] + H_2O \quad (3)$$

According to equation (2), in the presence of O_2 and NL-$MnCaO_2$, glucose is oxidized to gluconic acid and H_2O_2. Under the acidic condition, the generated H_2O_2, as a strong oxidant, can reduce AV and form peroxovanadium complex (a red-orange complex) with maximum absorption at 452 nm.

3.6. Study the repeatability and reproducibility

Repeatability and reproducibility are most important parameters to evaluate the application of biosensors, which can be determined from the relative standard deviation (RSD) or standard deviation (SD) of several measurements. To study the repeatability of the proposed system for determination of glucose, series of five solutions with the average glucose concentration of 200 μM were prepared and measurements were performed on the same day (during the same laboratory session). RSD% value was calculated to be 1.18%. The low RSD value (<1.9%) indicated a good repeatability of the proposed system for detection of glucose [59].

Moreover, biosensor reproducibility was studied by the five replicate measurements of the test solutions (with the average glucose concentration of 200 μM) during the five different days. The biosensor showed a reproducibility (RSD%) of 3.57%. This value is lower than 4% and the low RSD value (<4%) confirms that the measurements made with the proposed biosensor (NL-$MnCaO_2$) are reproducible [59].

3.7. Detection of glucose in human serum samples

To investigate the applicability and selectivity of the proposed enzyme-free glucose sensor, control assays were carried out in the presence of fructose, galactose and maltose (as glucose analogues). The concentration of these analogues was three times stronger than glucose. As shown in Fig. 6, the absorbance at 452 nm was negligible even at higher alternative substrate concentration, confirmed the high selectivity of the proposed system. In addition, the proposed system was used for the determination of glucose in spiked serum samples to evaluate the feasibility of the system. For this purpose, the human serum samples were spiked with different concentrations of glucose and the procedure described in section 2.5 was used for the determination of glucose concentration. The added-found procedure was applied to investigate the accuracy and precision of the proposed method for determination of glucose in serum samples. Table 2 shows the analysis results of glucose in the spiked serum sample. The results indicated that there is a good linear relationship between glucose concentration and absorbance intensity at 452 nm in the range of $(0–82.3) \times 10^{-6}$ M (0.9827). As shown in Table 2, the recoveries found and RSD values (for five replicates) for serum samples were in the range of 95.4–108.9% and 0.72–1.68%, respectively. The obtained detection limit (LOD) was 6.12×10^{-6} M. These results indicated the great potential of the proposed method for practical application and demonstrated that the developed method can be used as a sensitive, selective and enzyme-free method for detection of glucose in real samples.

4. Conclusion

In the current study, oxidase and glucose oxidase-like activities of NL-$MnCaO_2$ were investigated and an effective and enzyme-free platform for the detection of glucose and H_2O_2 was developed. The obtained results revealed pH and temperature dependence of the catalytic efficiency of the NL-$MnCaO_2$. These compounds can mimic oxidase activity at acidic condition (pH 5.0) and 25 °C. All these results indicated that NL-$MnCaO_2$ is a multi-functional enzyme mimetic nanostructure which can be used in various fields especially in the field of biomedicine. On the other hand, the determination of the blood glucose level is one of the most important medical issues. However, enzyme-based biosensors for the detection of glucose have some drawbacks. So, in the present work, we reported an enzyme free biosensor for the detection of glucose in real samples without significant interference from the matrix.

Declaration of competing interest

The authors declare that they have no known competing financial interests or personal relationships that could have appeared to influence the work reported in this paper.

CRediT authorship contribution statement

Samaneh Rashtbari: Data curation, Formal analysis, Methodology, Writing - original draft. **Gholamreza Dehghan:** Conceptualization, Project administration, Writing - review & editing. **Mojtaba Amini:** Validation, Investigation.

References

[1] A.G. Jarvis, L. Obrecht, P.J. Deuss, W. Laan, E.K. Gibson, P.P. Wells, et al., Enzyme activity by design: an artificial rhodium hydroformylase for linear aldehydes, Angew. Chem. Int. Ed. Engl. 56 (44) (2017) 13596–13600.
[2] P. Zhang, D. Sun, A. Cho, S. Weon, S. Lee, J. Lee, et al., Modified carbon nitride nanozyme as bifunctional glucose oxidase-peroxidase for metal-free bio-inspired cascade photocatalysis, Nat. Commun. 10 (1) (2019) 940.
[3] J. Wu, X. Wang, Q. Wang, Z. Lou, S. Li, Y. Zhu, et al., Nanomaterials with

enzyme-like characteristics (nanozymes): next-generation artificial enzymes (II), Chem. Soc. Rev. 48 (4) (2019) 1004–1076.
[4] H. Wei, E. Wang, Nanomaterials with enzyme-like characteristics (nanozymes): next-generation artificial enzymes, Chem. Soc. Rev. 42 (14) (2013) 6060–6093.
[5] P. Kumbhakar, S.S. Ray, A.L. Stepanov, Optical properties of nanoparticles and nanocomposites, J. Nanomater. (2014) 2014.
[6] I. Khan, K. Saeed, I. Khan, Nanoparticles: properties, applications and toxicities, Arabian J. Chem. 12 (7) (2019) 908–931.
[7] D. Teleanu, C. Chircov, A. Grumezescu, A. Volceanov, R. Teleanu, Impact of nanoparticles on brain health: an up to date overview, J. Clin. Med. 7 (12) (2018) 490.
[8] N. Bagheri, B. Habibi, A. Khataee, J. Hassanzadeh, Application of surface molecular imprinted magnetic graphene oxide and high performance mimetic behavior of bi-metal ZnCo MOF for determination of atropine in human serum, Atlanta 201 (2019) 286–294.
[9] W. He, W. Wamer, Q. Xia, J.-j. Yin, P.P. Fu, Enzyme-like activity of nanomaterials, J. Environ. Sci. Health C. 32 (2) (2014) 186–211.
[10] L. Gao, J. Zhuang, L. Nie, J. Zhang, Y. Zhang, N. Gu, et al., Intrinsic peroxidase-like activity of ferromagnetic nanoparticles, Nat. Nanotechnol. 2 (9) (2007) 577.
[11] J. Dong, L. Song, J.-J. Yin, W. He, Y. Wu, N. Gu, et al., Co3O4 nanoparticles with multi-enzyme activities and their application in immunohistochemical assay, ACS Appl. Mater. Interfaces 6 (3) (2014) 1959–1970.
[12] A. Asati, S. Santra, C. Kaittanis, S. Nath, J.M. Perez, Oxidase-like activity of polymer-coated cerium oxide nanoparticles, Angew. Chem. Int. Ed. Engl. 48 (13) (2009) 2308–2312.
[13] R. André, F. Natálio, M. Humanes, J. Leppin, K. Heinze, R. Wever, et al., V2O5 nanowires with an intrinsic peroxidase-like activity, Adv. Funct. Mater. 21 (3) (2011) 501–509.
[14] S.B. He, H.H. Deng, A.L. Liu, G.W. Li, X.H. Lin, W. Chen, et al., Synthesis and peroxidase-like activity of salt-resistant platinum nanoparticles by using bovine serum albumin as the scaffold, ChemCatChem 6 (6) (2014) 1543–1548.
[15] X. Liu, Q. Wang, H. Zhao, L. Zhang, Y. Su, Y. Lv, BSA-templated MnO 2 nanoparticles as both peroxidase and oxidase mimics, Analyst 137 (19) (2012) 4552–4558.
[16] W. He, H. Jia, X. Li, Y. Lei, J. Li, H. Zhao, et al., Understanding the formation of CuS concave superstructures with peroxidase-like activity, Nanoscale 4 (11) (2012) 3501–3506.
[17] A.K. Dutta, S.K. Maji, D.N. Srivastava, A. Mondal, P. Biswas, P. Paul, et al., Synthesis of FeS and FeSe nanoparticles from a single source precursor: a study of their photocatalytic activity, peroxidase-like behavior, and electrochemical sensing of H2O2, ACS Appl. Mater. Interfaces 4 (4) (2012) 1919–1927.
[18] Y. Jv, B. Li, R. Cao, Positively-charged gold nanoparticles as peroxidiase mimic and their application in hydrogen peroxide and glucose detection, Chem. Commun. 46 (42) (2010) 8017–8019.
[19] W. He, Y. Liu, J. Yuan, J.-J. Yin, X. Wu, X. Hu, et al., Au@ Pt nanostructures as oxidase and peroxidase mimetics for use in immunoassays, Biomaterials 32 (4) (2011) 1139–1147.
[20] W. He, X. Wu, J. Liu, X. Hu, K. Zhang, S. Hou, et al., Design of AgM bimetallic alloy nanostructures (M= Au, Pd, Pt) with tunable morphology and peroxidase-like activity, Chem. Mater. 22 (9) (2010) 2988–2994.
[21] X. Xia, J. Zhang, N. Lu, M.J. Kim, K. Ghale, Y. Xu, et al., Pd–Ir core–shell nanocubes: a type of highly efficient and versatile peroxidase mimic, ACS Nano 9 (10) (2015) 9994–10004.
[22] J. Wei, X. Chen, S. Shi, S. Mo, N. Zheng, An investigation of the mimetic enzyme activity of two-dimensional Pd-based nanostructures, Nanoscale 7 (45) (2015) 19018–19026.
[23] Y. Song, K. Qu, C. Zhao, J. Ren, X. Qu, Graphene oxide: intrinsic peroxidase catalytic activity and its application to glucose detection, Adv. Mater. 22 (19) (2010) 2206–2210.
[24] J.-W. Zhang, H.-T. Zhang, Z.-Y. Du, X. Wang, S.-H. Yu, H.-L. Jiang, Water-stable metal–organic frameworks with intrinsic peroxidase-like catalytic activity as a colorimetric biosensing platform, Chem. Commun. 50 (9) (2014) 1092–1094.
[25] C. Ray, S. Dutta, S. Sarkar, R. Sahoo, A. Roy, T. Pal, Intrinsic peroxidase-like activity of mesoporous nickel oxide for selective cysteine sensing, J. Mater. Chem. B 2 (36) (2014) 6097–6105.
[26] R. Singh, S. Singh, Role of phosphate on stability and catalase mimetic activity of cerium oxide nanoparticles, Colloids Surf. B Biointerfaces 132 (2015) 78–84.
[27] B. Fu, T. Liu, J. Chen, K. Li, CaF2 nanoparticles as peroxidase mimics for rapid and sensitive detection of aldosterone, Anal. Chim. Acta 1078 (2019) 119–124.
[28] L. Han, H. Zhang, D. Chen, F. Li, Protein-directed metal oxide nanoflakes with tandem enzyme-like characteristics: colorimetric glucose sensing based on one-pot enzyme-free cascade catalysis, Adv. Funct. Mater. 28 (17) (2018), 1800018.
[29] H. Zhang, X. Liang, L. Han, F. Li, "Non-Naked" gold with glucose oxidase-like activity: a nanozyme for tandem catalysis, Small 14 (44) (2018), 1803256.
[30] Y. Lin, J. Ren, X. Qu, Catalytically active nanomaterials: a promising candidate for artificial enzymes, Acc. Chem. Res. 47 (4) (2014) 1097–1105.
[31] X. Wang, Y. Hu, H. Wei, Nanozymes in bionanotechnology: from sensing to therapeutics and beyond, Inorg. Chem. Front. 3 (1) (2016) 41–60.
[32] M. Fernández-García, J.A. Rodriguez, Metal oxide nanoparticles, Encycl. Inorgan. Bioorgan. Chem. (2011).
[33] M. Amini, M.M. Najafpour, M. Zare, E. Amini, Nanolayered manganese-calcium oxide as an efficient and environmentally friendly catalyst for alcohol oxidation, J. Mol. Catal. Chem. 394 (2014) 303–308.
[34] M.M. Najafpour, M. Amini, D.J. Sedigh, F. Rahimi, M. Bagherzadeh, Activated layered manganese oxides with deposited nano-sized gold or silver as an efficient catalyst for epoxidation of olefins, RSC Adv. 3 (46) (2013) 24069–24074.
[35] F. Jiao, H. Frei, Nanostructured cobalt and manganese oxide clusters as efficient water oxidation catalysts, Energy Environ. Sci. 3 (8) (2010) 1018–1027.
[36] C.K. Remucal, M. Ginder-Vogel, A critical review of the reactivity of manganese oxides with organic contaminants, Environ. Sci. Process Impacts 16 (6) (2014) 1247–1266.
[37] H. Begum, M.S. Ahmed, S. Jeon, Ultra-fast and highly sensitive enzyme-free glucose biosensing on a nickel–nickel oxide core–shell electrode, RSC Adv. 7 (6) (2017) 3554–3562.
[38] B. Jiang, K. Zhou, C. Wang, Q. Sun, G. Yin, Z. Tai, et al., Label-free glucose biosensor based on enzymatic graphene oxide-functionalized tilted fiber grating, Sensor. Actuator. B Chem. 254 (2018) 1033–1039.
[39] S. Madhurantakam, J.B. Karnam, J.B.B. Rayappan, U.M. Krishnan, Enzyme-free monitoring of glucose utilization in stimulated macrophages using carbon nanotube-decorated electrochemical sensor, Appl. Nanosci. 7 (8) (2017) 773–780.
[40] R. Devasenathipathy, C. Karuppiah, S.-M. Chen, S. Palanisamy, B.-S. Lou, M.A. Ali, et al., A sensitive and selective enzyme-free amperometric glucose biosensor using a composite from multi-walled carbon nanotubes and cobalt phthalocyanine, RSC Adv. 5 (34) (2015) 26762–26768.
[41] N.S. Ridhuan, K.A. Razak, Z. Lockman, Fabrication and characterization of glucose biosensors by using hydrothermally grown ZnO nanorods, Sci. Rep. 8 (1) (2018), 13722.
[42] J. Zhang, X. Dai, Z.-L. Song, R. Han, L. Ma, G.-C. Fan, et al., One-pot enzyme-and indicator-free colorimetric sensing of glucose based on MnO2 nano-oxidizer, Sensor. Actuator. B Chem. 304 (1) (2020), 127304.
[43] T. Hou, T. Zhao, W. Li, F. Li, P. Gai, A label-free visual platform for self-correcting logic gate construction and sensitive biosensing based on enzyme-mimetic coordination polymer nanoparticles, J. Mater. Chem. B 5 (24) (2017) 4607–4613.
[44] J. Wang, Y. Hu, Q. Zhou, L. Hu, W. Fu, Y. Wang, Peroxidase-like activity of metal–organic framework [Cu (PDA)(DMF)] and its application for colorimetric detection of dopamine, ACS Appl. Mater. Interfaces 11 (47) (2019) 44466–44473.
[45] H. Li, H. Lin, X. Wang, W. Lv, F. Li, Dopamine-based paper analytical device for truly equipment-free and naked-eye biosensing based on the target-initiated catalyzed oxidation, ACS Appl. Mater. Interfaces 11 (40) (2019) 36469–36475.
[46] P.A. Nair, K. Sreenivasan, Non enzymatic colorimetric detection of glucose using cyanophenyl boronic acid included β-cyclodextrin stabilized gold nanoparticles, Anal. Methods 8 (9) (2016) 2082–2087.
[47] H.Y. Shin, S. Cho, M.I. Kim, Enzyme-free colorimetric detection of glucose using a composite entrapping gold and magnetic nanoparticles within an agarose gel matrix, J. Nanosci. Nanotechnol. 17 (11) (2017) 7971–7977.
[48] S. Adnan, N.H. Kalwar, M.W. Abbas, R.A. Soomro, M.A. Saand, F.R. Awan, et al., Enzyme-free colorimetric sensing of glucose using l-cysteine functionalized silver nanoparticles, SN Appl. Sci. 1 (2) (2019) 144.
[49] Y. Xiong, Y. Zhang, P. Rong, J. Yang, W. Wang, D. Liu, A high-throughput colorimetric assay for glucose detection based on glucose oxidase-catalyzed enlargement of gold nanoparticles, Nanoscale 7 (38) (2015) 15584–15588.
[50] W. Luo, C. Zhu, S. Su, D. Li, Y. He, Q. Huang, et al., Self-catalyzed, self-limiting growth of glucose oxidase-mimicking gold nanoparticles, ACS Nano 4 (12) (2010) 7451–7458.
[51] E.T. Rakitzis, P. Papandreou, Reactivity of 6-phosphogluconolactone with hydroxylamine: the possible involvement of glucose-6-phosphate dehydrogenase in endogenous glycation reactions, Chem. Biol. Interact. 113 (3) (1998) 205–216.
[52] M.H. Hadwan, S. kadhum Ali, New spectrophotometric assay for assessments of catalase activity in biological samples, Anal. Biochem. 542 (2018) 29–33.
[53] G. Dehghan, M. Shaghaghi, P. Alizadeh, A novel ultrasensitive and non-enzymatic "turn-on-off" fluorescence nanosensor for direct determination of glucose in the serum: as an alternative approach to the other optical and electrochemical methods, Spectrochim. Acta Mol. Biomol. Spectrosc. 214 (2019) 459–468.
[54] M. Amini, M.M. Najafpour, H. Naslhajian, E. Amini, S.M.F. Farnia, Nanolayered manganese–calcium oxide as an efficient catalyst toward organic sulfide oxidation, RSC Adv. 4 (21) (2014) 10851–10855.
[55] M.M. Najafpour, S. Nayeri, B. Pashaei, Nano-size amorphous calcium–manganese oxide as an efficient and biomimetic water oxidizing catalyst for artificial photosynthesis: back to manganese, Dalton Trans. 40 (37) (2011) 9374–9378.
[56] M.M. Najafpour, K.C. Leonard, F.-R.F. Fan, M.A. Tabrizi, A.J. Bard, C.K. King'Ondu, et al., Nano-size layered manganese–calcium oxide as an efficient and biomimetic catalyst for water oxidation under acidic conditions: comparable to platinum, Dalton Trans. 42 (14) (2013) 5085–5091.
[57] K. Princy, A. Gopinath, Optimization of physicochemical parameters in the biofabrication of gold nanoparticles using marine macroalgae Padina

tetrastromatica and its catalytic efficacy in the degradation of organic dyes, J. Nanostructure Chem. 8 (3) (2018) 333–342.
[58] X. Cao, Y. Li, Z. Zhang, J. Yu, J. Qian, S. Liu, Catalytic activity and stability of glucose oxidase/horseradish peroxidase co-confined in macroporous silica foam, Analyst 137 (24) (2012) 5785–5791.
[59] M. Artigues, J. Abellà, S. Colominas, Analytical parameters of an amperometric glucose biosensor for fast analysis in food samples, Sensors 17 (11) (2017) 2620.
[60] L. Han, C. Li, T. Zhang, Q. Lang, A. Liu, Au@ Ag heterogeneous nanorods as nanozyme interfaces with peroxidase-like activity and their application for one-pot analysis of glucose at nearly neutral pH, ACS Appl. Mater. Interfaces 7 (26) (2015) 14463–14470.
[61] C. Jiang, J. Zhu, Z. Li, J. Luo, J. Wang, Y. Sun, Chitosan–gold nanoparticles as peroxidase mimic and their application in glucose detection in serum, RSC Adv. 7 (70) (2017) 44463–44469.
[62] T.G. Choleva, V.A. Gatselou, G.Z. Tsogas, D.L. Giokas, Intrinsic peroxidase-like activity of rhodium nanoparticles, and their application to the colorimetric determination of hydrogen peroxide and glucose, Mikrochim. Acta 185 (1) (2018) 22.
[63] Z. Wang, S. Liu, P. Wu, C. Cai, Detection of glucose based on direct electron transfer reaction of glucose oxidase immobilized on highly ordered polyaniline nanotubes, Anal. Chem. 81 (4) (2009) 1638–1645.
[64] M. Ashrafi, A. Salimi, A. Arabzadeh, Photoelectrocatalytic enzymeless detection of glucose at reduced graphene oxide/CdS nanocomposite decorated with finny ball CoOx nanostructures, J. Electroanal. Chem. 783 (15) (2016) 233–241.
[65] H. Zhai, T. Feng, L. Dong, L. Wang, X. Wang, H. Liu, et al., Development of dual-emission ratiometric probe-based on fluorescent silica nanoparticle and CdTe quantum dots for determination of glucose in beverages and human body fluids, Food Chem. 204 (1) (2016) 444–452.
[66] D. Jampaiah, T.S. Reddy, V.E. Coyle, A. Nafady, S.K. Bhargava, Co 3 O 4@ CeO 2 hybrid flower-like microspheres: a strong synergistic peroxidase-mimicking artificial enzyme with high sensitivity for glucose detection, J. Mater. Chem. B 5 (4) (2017) 720–730.
[67] F. Qiao, L. Chen, X. Li, L. Li, S. Ai, Peroxidase-like activity of manganese selenide nanoparticles and its analytical application for visual detection of hydrogen peroxide and glucose, Sensor. Actuator. B Chem. 193 (2014) 255–262.
[68] H. Wei, E. Wang, Fe3O4 magnetic nanoparticles as peroxidase mimetics and their applications in H2O2 and glucose detection, Anal. Chem. 80 (6) (2008) 2250–2254.
[69] C.-P. Huang, S.-W. Liu, T.-M. Chen, Y.-K. Li, A new approach for quantitative determination of glucose by using CdSe/ZnS quantum dots, Sensor. Actuator. B Chem. 130 (1) (2008) 338–342.
[70] N.S. Vallabani, A.S. Karakoti, S. Singh, ATP-mediated intrinsic peroxidase-like activity of Fe3O4-based nanozyme: one step detection of blood glucose at physiological pH, Colloids Surf. B Biointerfaces 153 (2017) 52–60.